Amelioration of experimental autoimmune myocarditis through activation of invariant natural killer T cells by administration of α-galactosylceramide

Kazuhisa Yoshino,[1] Masashi Satoh,[2,3] Toshitsugu Iwayama,[2] Shusaku Kobayashi,[2]
Hirotsugu Okamoto,[4] Koji Eshima,[2,3] Hiroshi Watarai,[5,6] Kazuya Iwabuchi[2,3]

[1] Program in Anesthesiology, Kitasato University Graduate School of Medical Sciences
[2] Program in Cellular Immunology, Kitasato University Graduate School of Medical Sciences
[3] Department of Immunology, Kitasato University School of Medicine
[4] Department of Anesthesiology, Kitasato University School of Medicine
[5] Division of Stem Cell Cellomics, Institute of Medical Sciences, The University of Tokyo
[6] Department of Immunology and Stem Cell Biology, Faculty of Medicine, Institute of Medical Pharmaceutical and Health Sciences, Kanazawa University

Background: NKT cells recognize glycolipid antigens such as α-GC in the context of the CD1d molecule and play an ameliorating role by producing immunoregulatory cytokines in models of ischemic heart disease, e.g., acute myocardial infarction and ischemia/reperfusion injury.
Objective: To examine whether iNKT cells also play ameliorating role for EAMC, α-GC was administered to activate iNKT cells at the time of immunization for induction of EAMC.
Methods: EAMC was induced in BALB/c mice or iNKT-deficient TRAJ18^{-/-} mice by immunizing subcutaneously with a peptide (residue 614-629) of mouse cardiac myosin heavy chain-α emulsified with Complete Freund's Adjuvant followed by additional immunization on day 7. Vehicle or α-GC was administered as a mixture of the first immunizing emulsion. Three weeks later, histological and gene-expression analyses were performed to examine the effects.
Results: The mice inoculated with α-GC for immunization showed reduced TNF-α and increased IL-10 (interleukin-10) expression, with fewer infiltrated inflammatory cells. Accordingly, the fibrotic lesion area was reduced in the heart. EAMC induced in iNKT-cell deficient mice was aggravated in comparison with that induced in BALB/c mice with an enhanced fibrotic lesion area on day 21 after immunization.
Conclusion: The presence of iNKT cells and activation of iNKT cells on immunization ameliorated the inflammation of EAMC.

Abbreviations: NKT, natural killer T; α-GC, α-galactosylceramide; iNKT, invariant NKT; EAMC, experimental autoimmune myocarditis; TNF-α, tumor necrosis factor-α; TCR, T-cell antigen receptor; Ag, antigen; AMI, acute myocardial infarction; Treg, regulatory T; MyHC-α, cardiac myosin heavy chain α-isoform; PTX, Bordetella pertussis toxin; CFA, Complete Freund's Adjuvant; PBS, phosphate buffered saline; H&E, hematoxylin and eosin; dLN, draining lymph node; APC; antigen-presenting cell; PCR, polymerase chain reaction; Mϕ, macrophages; Mo, monocytes; CMNC, cardiac mononuclear cell; LPC, ligand presenting cell; CD, cluster of differentiation; DC, dendritic cells; ICD, International Statistical Classification of Diseases and Related Health Problems Ninth Revision; I/R, ischemia/reperfusion; IL, interleukin; mAb, monoclonal antibody; MFI, mean fluorescence intensity

Introduction

Myocarditis has been defined as "the presence of cellular inflammatory infiltrate in direct association with necrosis or degeneration of myocytes not typical of ischemic necrosis" accompanied with cardiac dysfunction.[1] The causes of myocarditis include infections by viruses, bacteria, fungi, and parasites, cardiotoxic drug-induced, autoimmunity-related, and others that are recapitulated as idiopathic.[2] The prevalence of cases worldwide is estimated to be approximately 22/100,000/year according to the ICD-9 codes.[3] Myocarditis is one of the causes of sudden death (12%) among juvenile and adolescent population with a prevalence of 1/200,000/year.[4] However, the severity of the disease is variable with minimal symptoms that make it difficult to diagnose lethal cases that are accompanied with severe myocardial damage that result in fetal arrhythmia and cardiogenic shock, which makes the prevalence underestimated.[5]

The myocardial damage and the resultant loss of cardiomyocytes due to any etiology are filled primarily with fibroblasts and compensated by hypertrophy of surviving cardiomyocytes. The process of cardiac remodeling, for repairing damaged cardiac muscles and compensation of cardiac function, often results in heart failure causing fatalities.[6,7] Moreover, because the causes and development are variable, it is difficult to effectively control the inflammation and remodeling processes.[2,8] Therefore, the prevention and effective therapeutics for myocarditis and cardiac remodeling must be developed.

NKT cells are a subset of T cells that are restricted by the CD1d molecule.[9] The majority of NKT cells express the invariant TCR α chain (TRAV11AJ18) and are classified as type I NKT or iNKT cells. iNKT cells recognize glycolipid Ag such as α-GC and exhibit various functions as exemplified as a Swiss-army knife.[10] iNKT cells are able to function not only as effector cells that exhibit cytocidal activity through perforin and Fas ligands but also as regulatory cells through production of IL-10 and tumor growth factor-β in immune responses.[10] Accordingly, iNKT cells have been shown to modulate disease progression in various disease models to date.[11,10]

NKT cells have been reported to be recruited to infarcted lesions following AMI model in mice and to ameliorate the cardiac remodeling upon activation with α-GC.[13] Furthermore, the beneficial effect of iNKT cells has been reported in cardiac remodeling following ischemia/reperfusion injury models in mice.[14] Regarding EAMC models, it has been reported with BALB/c mice immunized with purified protein of porcine cardiac myosin that α-GC administration ameliorated the inflammation.[15] Although a single dose of α-GC as an immunization ameliorated the myocarditis with increased NKT cells and Treg cells, the involvement of NKT cells in this particular model and the relation with Treg cells remained elusive. Thus, we examined the effect of NKT-cell activation to mitigate EAMC in BALB/c mice and investigated a possible mechanism for amelioration.

Materials and Methods

Mice

Male and female, 6-week-old BALB/c mice were purchased from CLEA Japan, (Tokyo) and TRAJ18 gene (prepared by CRISPR/Cas9 gene editing; Traj18$^{-/-}$)[16] mice were obtained from the Institute of Medical Sciences, The University of Tokyo, and were maintained at the Animal Facility in Kitasato University School of Medicine. The mice were maintained on food and water *ad libitum* with a 12-hour light/12-hour dark cycle, treated humanely, and housed in specific pathogen-free conditions at the Animal Facility in Kitasato University School of Medicine. All the experimental procedures on the mice conformed to the Animal Experimentation and Ethics Committee of the Kitasato University School of Medicine (2016-109, 2017-143, 2018-118, -119, 2019-024, -025).

Reagents

The authentic peptide residue 614-629 of mouse MyHC-$\alpha_{614-629}$ (Ac-SLKLMATLFSTYASAD)[17] and the modified form of MyHC-$\alpha_{614-629}$ with arginine residues (**R**) at both amino (N)-terminal and carboxy (C)-terminal ends (MyHC-$\alpha_{614-629}$**R**: Ac-**R**SLKLMATLFSTYASAD**R**) that do not appear in the original sequence of MyHC-α[18] were synthesized and purchased from Sigma-Genosys Japan (Ishikari) and Hokkaido System Science (Sapporo). Purified PTX was purchased from Sigma-Aldrich (St. Louis, MO, USA). CFA was purchased from Calbiochem-Sigma Aldrich (global) and *Mycobacterium tuberculosis* strain H37Ra from Difco (Detroit, MI, USA). α-GC was purchased from Funakoshi (Tokyo) or provided by Wako Pure Chemical Industries (Osaka).

Induction of EAMC in mice and administration of NKT-ligands with inoculum

To induce EAMC, MyHC-$\alpha_{614-629}$ or MyHC-$\alpha_{614-629R}$ (100 μg) was emulsified in CFA (1:1 v/v) containing 5 mg/ml *Mycobacterium tuberculosis* H37Ra (Difco) and a total of 200 μl of the emulsion was subcutaneously injected in the upper and lower parts of the back.[17,18] When mice were treated with the NKT-cell ligand, α-GC

for the experimental group or the vehicle for the control group was included in the immunization inoculum as 2 μg of α-GC or the vehicle/200 μl/mouse in the first immunization.[19] Concurrent with immunization, 0.2 μg of PTX in 100 μl of PBS was injected intraperitoneally as an additional adjuvant. The second immunization of MyHC-α peptide/CFA emulsion without α-GC was given 7 days later.

Histopathological evaluation of EAMC
For histopathological scoring, 21 days after immunization, when the inflammation usually peaks, after euthanasia, the hearts were obtained. The cardiac tissues were fixed in 10% phosphate-buffered formaldehyde solution. Fixed tissues were embedded in paraffin, sectioned in 10-μm-thick slices, and stained with the standard method for H&E to evaluate the infiltration of inflammatory cells or Masson's trichrome staining to quantify the fibrotic area in the cardiac tissue. Microscopic images were observed and incorporated with a BIOREVO microscope (BZ-9000; Keyence, Osaka), integrated with tiling, and analyzed with BZII software (Keyence).

Preparation of single cell suspensions from the immunized mice
Mice were deeply anesthetized with isoflurane, bled, and euthanized. Thereafter, the hearts were perfused with PBS (-) [PBS (-); NaCl 154 mM, Na2HPO4 5.6 mM, KH2PO4 1.06 mM; pH 7.4] to wash out the blood and removed for further analyses including histopathology, gene expression, and flow cytometry. Excised hearts were cut into pieces and digested with collagenase D (2 mg/ml) and DNase I (0.4 mg/ml) (Roche Diagnostics, Tokyo) at 37℃ for 1 hour with gentle shaking. The digests were rendered to go through mesh to remove cell debris, centrifuged, and washed several times to obtain cardiac mononuclear cells.[20] Single cell suspensions of lymph node and spleen cells were prepared by gentle homogenization, and the spleen cell suspensions were treated with hemolysis buffer to remove erythrocytes.

Quantification of serum level of creatine kinase and cardiac troponin I
Creatine kinase concentrations in sera were quantified by colorimetric assays using DRI-CHEM 7000 V (FUJIFILM, Tokyo) according to the manufacturer's protocol. The level of cardiac troponin I (cTnI) in sera was quantified by the High Sensitivity Mouse Cardiac Troponin-I ELISA kit (Life Diagnostics, West Chester, PA, USA) according to the manufacturer's protocol.

Flow cytometric analyses
The cells were incubated with 2.4G2 mAb (anti-Fcγ RIII/II) to block non-specific binding of primary mAb and then stained with combinations of various specific mAbs. Stained cells were acquired with FACS Verse or FACS Aria flow cytometers (BD Bioscience, San Jose, CA, USA) and analyzed with FlowJo software (Tree Star, Ashland, OR, USA). Any and all 7-aminoactinomycin D (7-AAD; BD Bioscience) positive cells were electronically gated as dead cells from the analysis. Anti-mouse mAbs used in this study were as follows. APC-conjugated mAb: anti-CD11b (M1/70, BioLegend, San Diego, CA, USA), anti-CD11c (N418, BioLegend), anti-CD103 (αE integrin; 2E7, BioLegend), anti-CD115 (CSF1R; AFS98, BioLegend), anti-Ly6C (HK1.4, BioLegend), anti-CD169 (Siglec-1; 3D6.112, BioLegend), and anti-Feeder Cells (MEFSK4, Miltenyi Biotec). APC/Cy7-conjugated mAb: antiCD45 (30-F11, BioLegend) and anti-TCRβ (H57-597, BioLegend). Brilliant Violet-conjugated mAb: anti-F4/80 (BM8, BioLegend Japan, Tokyo). FITC-conjugated mAb: anti-Ly-6C (HK1.4, BioLegend, San Diego), anti-CD206 (C068C2, BioLegend), anti-CD86 (GL1, BD), anti-CD206 (C068C2, BioLegend), anti-CX3CR1 (SA011F11, BioLegend), anti-CD80 (16-10A1,BD), and anti-CD31 (390, BioLegend). Phycoerythrin (PE)-conjugated mAb: PE-anti-CD1d (1B1, BioLegend), PE-anti-Ly6G (1A8, BioLegend), anti-MERTK (2B10C42), anti-MHC-II (I-A^{d}) (NIMR-4, eBioscience), anti-ICOSL (CD275) (B7H2, BioLegend), anti-CCR2 (CD192) (SA203G11, BioLegend), and anti-CD210 (IL-10Rα; 1B1.3a, BioLegend). PE/Cy7-conjugated mAb: anti-CD11b (M1-70, BioLegend). APC-labeled α-GC-loaded tetramer and unloaded CD1d-tetramer for analyses of iNKT cells were provided by the National Institutes of Health Tetramer Core Facility at Emory University (Atlanta, GA, USA).[19,21]

Proliferative responses and cytokine production upon antigen stimulation
dLN cells were obtained from mice 10 days after immunization and were used with the T-cell Recovery Kit (Cedarlane, Ontario, Canada) according to the manufacturer's protocol. The dLN cells were incubated with reagents supplied in the kit and applied to recovery columns to obtained T-enriched cells as flow through fractions. T cells (2×10^5) from each group were cultured in complete medium (RPMI [Roswell Park Memorial Institute]-1640) (Sigma), supplemented with 10% heat-inactivated fetal calf serum, 100 U/ml penicillin, 100 μg/

ml streptomycin, and 50 μM β-mercaptoethanol with irradiated splenocytes (1×10^5) as APC in the presence of MyHC-α peptides (0.01$-$1 μg/ml) for 3 days. The spleen cells for APC were enriched for dendritic cell fractionation by preparing the cells in the interface of density centrifugation with 55% Percoll.[22] The concentration of cytokines was quantified in the supernatant of the above culture by a CBA (cytometric bead array) kit (BD Bioscience) according to the manufacturer's protocol with a flow cytometer. For proliferation assay, cells of the above setup in culture plates were then pulse-labeled with ³H-thymidine (³H-TdR; 0.5 μCi/well) for the following 16 hours. The ³H-TdR incorporation of each well was quantified with a liquid scintillation counter.

PCR

Total RNA was extracted from either prepared suspension of single cells from each tissue or a part of excised piece of cardiac tissue using TRIzol reagent (Life Technologies) and with shaker homogenizer for a tissue piece (heart). cDNA was synthesized with 1 μg of total RNA by PrimeScript RT Master Mix (Takara Bio, Shiga). Synthesized cDNA was diluted appropriately with water and used as a template for subsequent quantitative PCR. Quantitative PCR was performed with SYBR Premix Ex

Taq II (Takara Bio) and CFX96/384 (Bio-Rad, Hercules, CA, USA) according to the manufacturer's protocols. Target gene expression was normalized by β-actin and calculated by the 2-$\Delta\Delta$CT method. Primers were as follows:

|		
actb	forward	5'-GGCTGTATTCCCCTCCATCG-3'
	reverse	5'-CCAGTTGGTAACAATGCCATGT-3'
tnfa	forward	5'-GCCACCACGCTCTTCTGTCTAC-3'
	reverse	5'-GGGTCTGGGCCATAGAACTGAT-3'
acta2	forward	5'-AAGAGGAAGACAGCACAGCC-3'
	reverse	5'-AGCGTCAGGATCCCTCTCTT-3'
col1a1	forward	5'-CCAGCCGCAAAGAGTCTACA-3'
	reverse	5'-CATACCTCGGGTTTCCACGT-3'
col3a1	forward	5'-GCGAGCGGCTGAGTTTTATG-3'
	reverse	5'-TAGGACTGACCAAGGTGGCT-3'
il10	forward	5'-GCTCTTACTGACTGGCATGAG-3'
	reverse	5'-GCGAGCTCTAGGAGCATGTG-3'
ccl2	forward	5'-CCCAATGAGTAGGCTGGAGA-3'
	reverse	5'-GCTAAGACCTTAGGGCAGA-3'
cd1d1	forward	5'-ACTCAGCCACCATCAGCTTC-3'
	reverse	5'-AGGGTACATTTCACAGCCCG-3'
cxcl16	forward	5'-CCTTGTCTCTTGCGTTCTTCC-3'
	reverse	5'-TCCAAAGTACCCTGCGGTATC-3'
il17	forward	5'-TGAAGGCAGCAGCGATCA-3'
	reverse	5'-GGAAGTCCTTGGCCTCAGTGT-3'
il4	forward	5'-GTTGTCATCCTGCTCTTCTTTCTC-3'
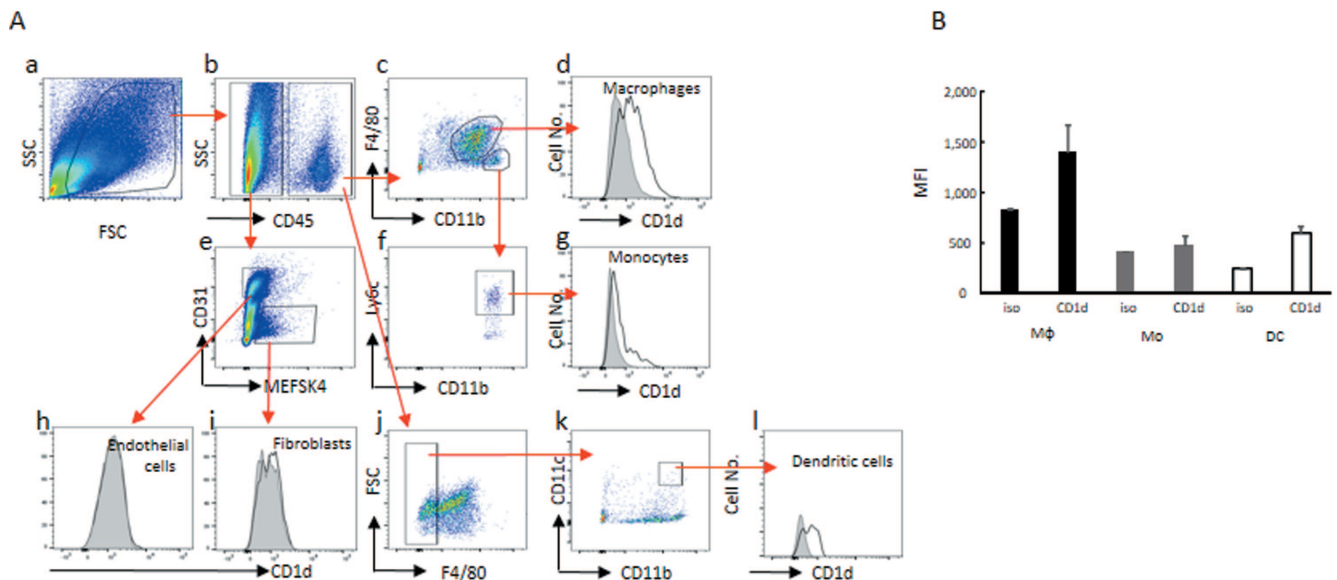
Figure 1. The F4/80⁺CD11b⁺ fraction is the main CD1d-expressor in the heart.

Cardiac mononuclear cells were prepared by digestion of the heart tissue with collagenase D and DNase I and analyzed with flow cytometer as described in the Materials and Methods. **A**. Flow cytometric profiles. a. Forward scatter (FSC) vs. Side scatter (SSC) plot. b. CD45 vs. SSC plot. c. CD11b vs. F4/80 plot. e. MEFSK4 vs. CD31 plot. f. CD11b vs. Ly6C plot. j. F4/80 vs. FSC plot. k. CD11b vs. CD11c plot. Panels (d, g, h, i, l) of CD1d histogram of macrophage (d. Mϕ; CD11b⁺F4/80ʰⁱ), monocyte (g. Mo; CD11b⁺Ly6C⁺), endothelial cell (h. MEFSK4⁻CD31⁺), cardiac fibroblast (i. MEFSK4⁺CD31⁻) and dendritic cell (l. DC; CD11b⁺CD11c⁺). **B**. Mean fluorescence intensity (MFI) of CD1d staining of each population, Mϕ (black column), Mo (gray column), and DC (white column). Representative results of at least five independent experiments (n = 3$-$4 mice/time) were shown. Graph data are shown as mean $\pm$ SD.

reverse   5'-CACAGCAACGAAGAACACCAC-3'
ifng   forward   5'-TCAAGTGGCATAGATGTGGAAGAA-3'
reverse   5'-TGGCTCTGCAGGATTTTCATG-3'

Statistical analyses

Data are shown as mean $\pm$ standard deviation (SD). Statistical analysis between two groups was performed by Student's t-test and among three groups was performed using ANOVA followed by Tukey-Kramer tests. Values with P < 0.05 were considered statistically significant. The significance (P < 0.05) of the difference between two mean clinical scores was determined by the non-parametric Mann-Whitney *U*-test for comparison of two independent populations.

Results

CD1d expressing cells in the heart

First to examine CD1d^{+} cells that are capable to present α-GC to iNKT cells in the heart, CD1d expression was analyzed on cardiac mononuclear cells obtained from BALB/c mice. Figure 1 shows a scheme of gating strategy to analyze each population for the expression of CD1d according to previous report.[18,20] The CD45^{+} cells were further separated with the expression of CD11b and F4/80 to detect Mϕ (Figure 1Ab,c,d). In a similar way, the CD11b^{+}F4/80^{lo} fraction were further developed CD11b^{+}Ly6C^{hi} to detect Mo (Figure 1Ab,c,f,g). The F4/80^{-} fraction of CD45^{+} cells was separated with the expression of CD11b and CD11c to detect DC (Figure 1Ab,j,k,l). Although these 3 populations were positive for CD1d expression (Figure 1Ad,g,l), Mϕ exhibited the highest MFI in CD45^{+} cells in the heart (Figure 1B). Meanwhile, the CD45^{-} fraction of cells was separated with MEFSK4 and CD31 to detect cardiac endothelial cells (CD31^{+}MEFSK4^{-}; Figure 1Ae,h) and cardiac fibroblasts (CD31^{-}MEFSK4^{+}; Figure 1 Ae,i) was both negative for CD1d.
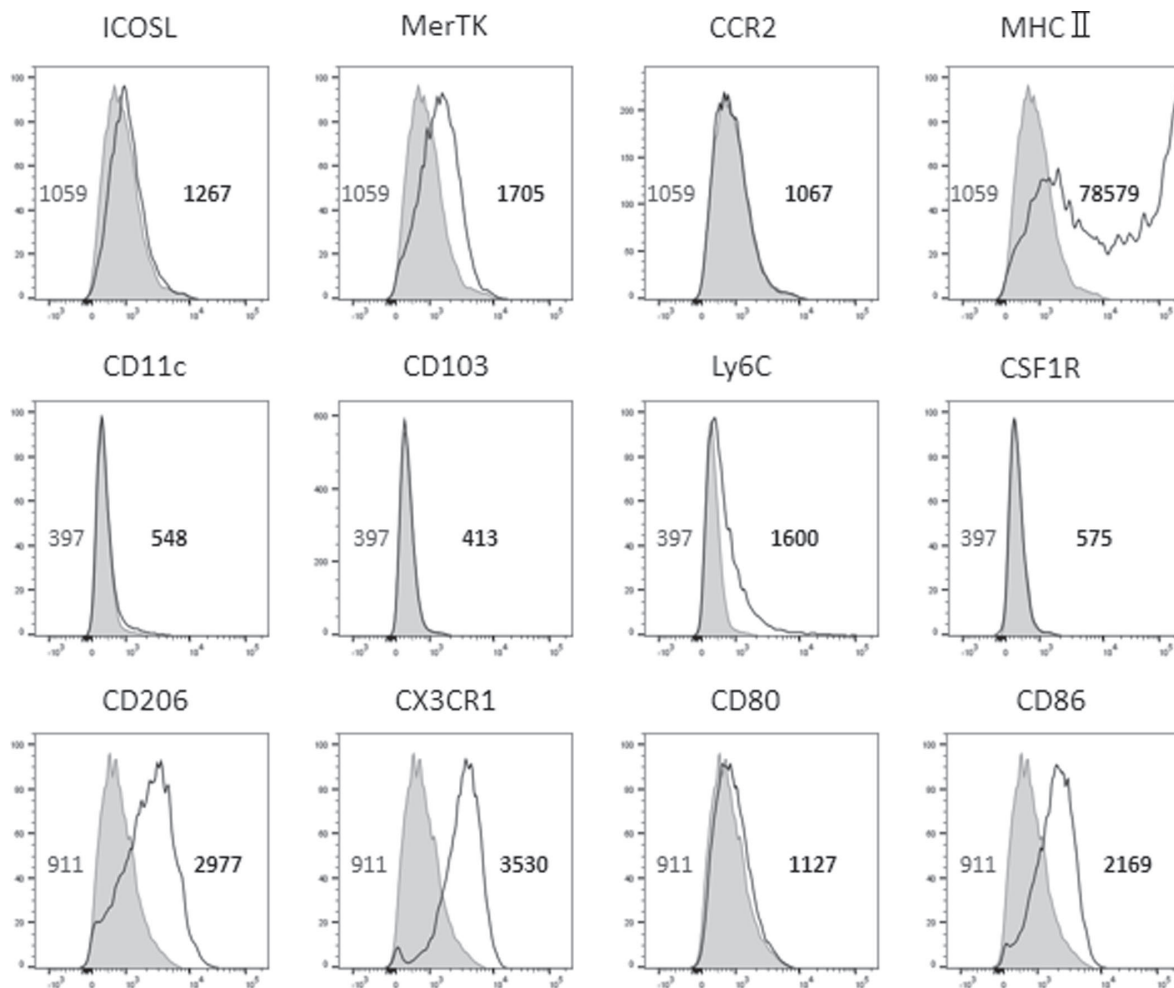

Figure 2. Expression of surface markers on F4/80^{+}CD11b^{+} cardiac Mϕ in untreated BALB/c mice

Cardiac mononuclear cells were stained with F4/80/CD11b indicated mAb and the results were expressed as a histogram. Numbers in the histogram panels represent MFI of isotype control (gray) or indicated mAb staining (black).
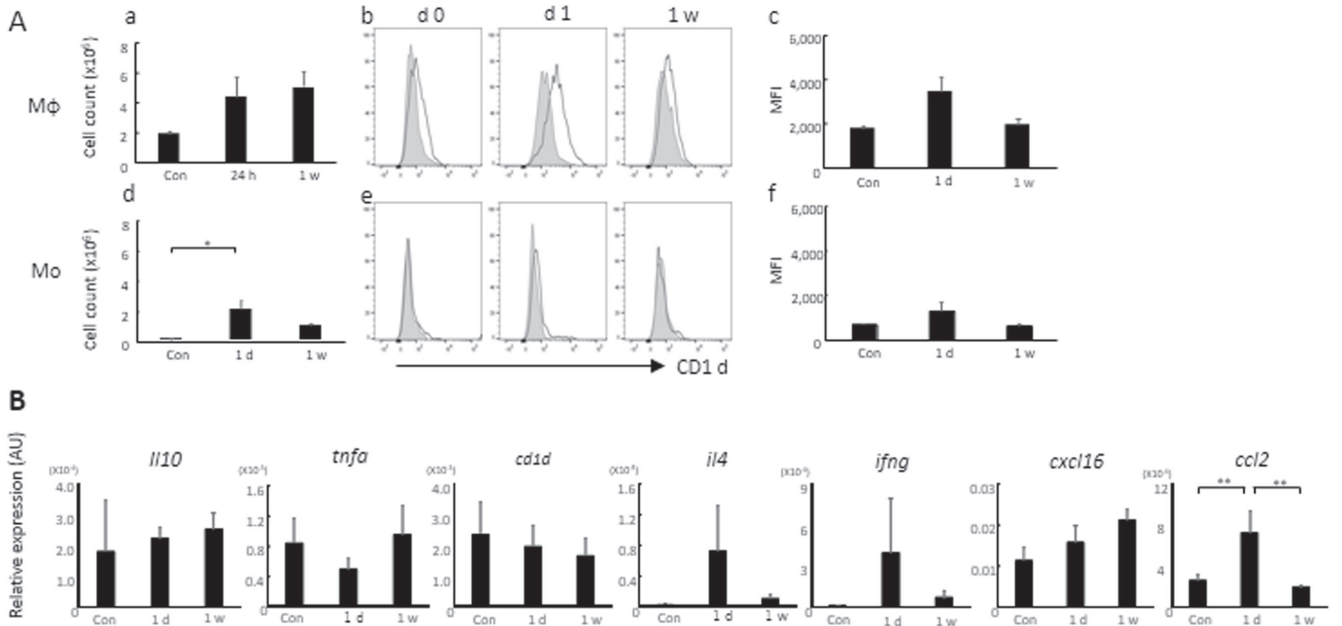
Figure 3. Cellular responses of antigen presenting cells and NKT cells in the heart tissue before, at 1 day, and 1 week after intraperitoneal administration of α-GC

A. Cell counts (a,d), CD1d expression (b,e), and MFI of CD1d staining (c,f) of Mϕ (a,b,c) or Mo (d,e,f), respectively at each time point.
B. Gene expression by iNKT cells with quantitative PCR analyses for indicated genes before and after administration of α-GC at each time point. (n = 3 mice for each group. Representative of two independent experiments with similar results were shown. Graph data are shown as mean $\pm$ SD. *P < 0.05, **P < 0.01
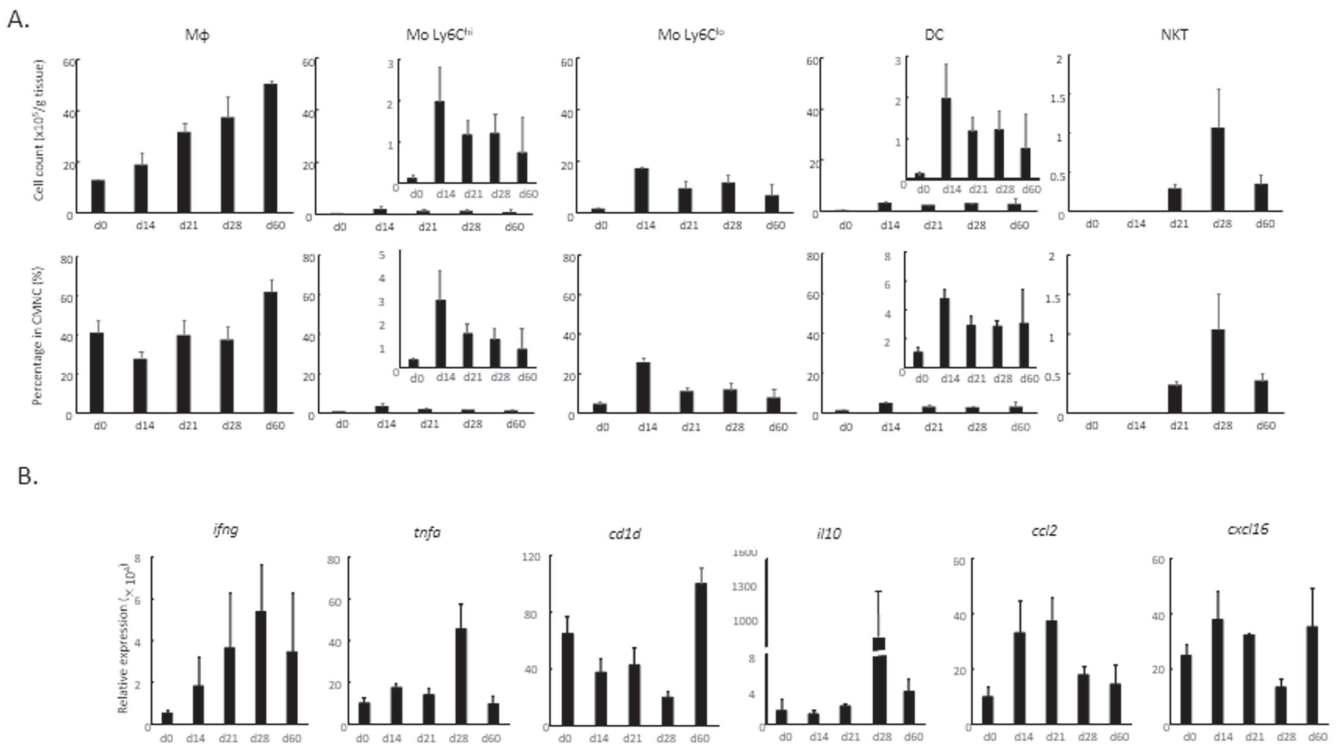

Figure 4. Cellular dynamics and gene expressions in the heart tissue at each time point

A. Upper panels: cell count/g tissue of the indicated subset of cells in the hearts at days 0, 14, 21, 28, and 60 after immunization with α-GC. Lower panels: Percentages of cells in the cardiac mononuclear cells obtained from the heart tissue at the same time as those in the upper panels. Inset is demonstrated with different numerical values in the y-axis to better depict fluctuations. **B**. Expressions of genes indicated in each panel at each time point as above (**A**). Three mice for each time point were analyzed. Representatives of two independent experiments with similar results are shown. Graph data are shown as mean $\pm$ SD.
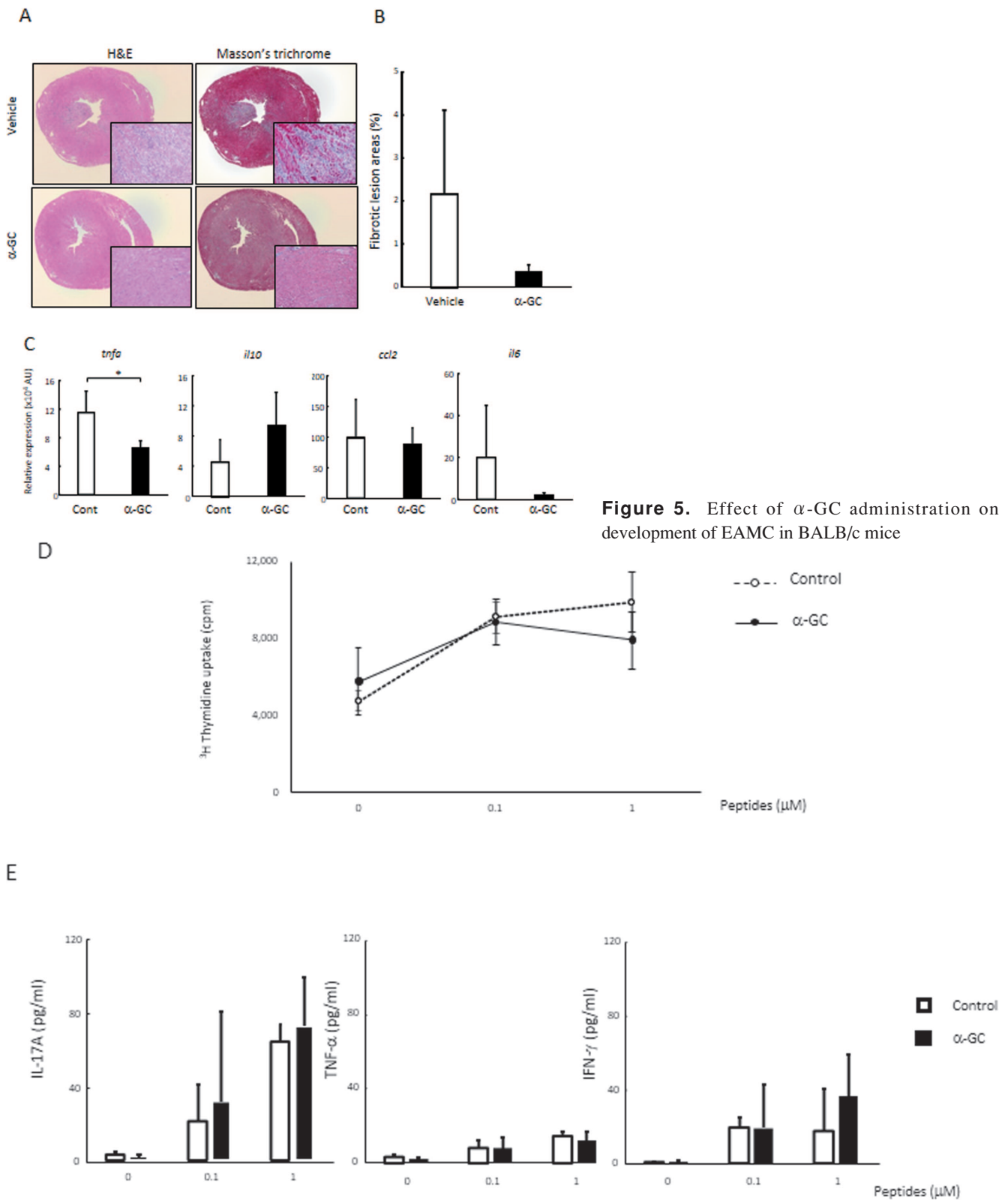
A

H&E   Masson's trichrome

Vehicle

α-GC

B

Fibrotic lesion areas (%)

Vehicle   α-GC

C

tnfa   il10   ccl2   il6

Relative expression [×10⁴ AU]

Cont   α-GC

Figure 5. Effect of α-GC administration on development of EAMC in BALB/c mice

D

³H Thymidine uptake (cpm)

Peptides (μM)

--o-- Control
—●— α-GC

E

IL-17A (pg/ml)   TNF-α (pg/ml)   IFN-γ (pg/ml)

Peptides (μM)

☐ Control
■ α-GC

A. Histopathology of the heart tissue obtained from mice administered vehicle or α-GC and stained with H&E or Masson's trichrome solution. Magnification $\times$5, Inset $\times$20. **B**. Fibrotic lesion areas of mice administered vehicle or α-GC. **C**. Expression of genes indicated in each panel of the heart tissue in comparison with vehicle- or α-GC-treated mice (n = 5 for control group, n = 4 for α-GC administration group). **D**. Proliferative response of T cells obtained from dLN (draining lymph node) of EAMC-induced mice (n = 3 for each group) with vehicle (control) or α-GC administration (α-GC) after 21 days of primary immunization. T-enriched cells were cultured at each concentration of MyHC-α peptide in the presence of antigen-presenting cells (APCs) as described in **Materials and Methods**. ³H-TdR incorporation by T cells at each concentration of MyHC-α peptide was quantified with scintillation counter. **E**. Cytokine concentration in culture supernatant (pg/ml). The concentration of IFN-γ, TNF-α, and IL-17 was quantitated in triplicate culture. Representative data of three independent experiments with similar results are shown. Graph data are shown as mean $\pm$ SD. *P < 0.05

The expression of other surface markers of F4/80⁺CD11b⁺ cardiac Mφ

To explore other surface markers on cardiac Mφ, F4/80⁺CD11b⁺ cells were further stained with anti-mouse mAb and analyzed with flow cytometer (Figure 2). Cardiac Mφ was clearly positive for MerTK, MHC class II (mixed population of low and high), CD86, CD206 (macrophage mannose receptor; CLEC13D), CX₃CR1; weakly positive for CD80; minimally positive to negative for ICOSL (CD275), CCR2 (CD192), CD11c, CD103 (α_E integrin), and CD115 (CSF1R); and presumably a fraction of cells are positive for Ly6C in steady state. Regarding other markers not included in Figure 2, CD169 (Sialoadhesin, Siglec-1) was negative and CD210 (IL-10R-α) was weakly positive (data not shown).

Cellular responses after α-GC administration

To examine cellular responses and dynamics in the heart following administration of α-GC, the main CD1d⁺ cells in the heart, cardiac macrophages (Mφ) and monocytes (Mo) were analyzed. The Mφ exhibited an increase in cell counts, and the MFI level of CD1d expression one day (day 1) after α-GC administration and the cell counts stayed at a similar level at 1 week as that of day 1; whereas the MFI of CD1d returned to the control level at 1 week (Figure 3Aa,b,c). On the other hand, Mo exhibited the marked increase of cell counts at day 1 but appeared to be in a decreasing trend. The up-regulation in MFI of CD1d was observed at day 1 after α-GC administration but appeared minimal compared to that of Mφ (Figure 3Ad,e,f). When the expression of indicated genes was analyzed, those of *il4*, *ifng*, and *ccl2* that are presumably produced by NKT cells appeared to be up-regulated at day 1 and returned to control level at 1 week (Figure 3B). Meanwhile, the expression of *cxcl16* appeared to gradually increase, but the other genes did not exhibit distinct patterns.

Analyses of cellular dynamics and gene expression in the hearts of mice-induced EAMC: a kinetic study

Dynamics of CMNC obtained from cardiac digests and gene expression of the heart were analyzed with flow cytometer or with real time PCR at each time point (days 0, 14, 21, 28, 60) in mice that were induced EAMC. The number of cardiac Mφ gradually increased after induction to day 60, whereas those of Mo showed a small peak at day 14 and then appeared to decrease, which similarly observed in both Ly6C^hi and Ly6C^lo population as shown in inset. Notably, the number of cells appeared about ten times more for Ly6C^lo compared to that of Ly6C^hi population (Figure 4A *upper panel/inset*). As for DC,

the kinetics was similar to that of Mo as shown in inset figure, though the numbers were smaller than Mφ and Mo fractions. The ratio to the total mononuclear cells obtained from the heart appeared to reflect the dynamics (Figure 4A *lower panel*). There seemed a decrease in the ratio of Mφ at day 14 presumably due to an increase of Ly6C^lo Mo. Of note, iNKT cells appeared to be detected at day 21, peaked at day 28 and decreased to the level of day 21 at day 60. This tendency was reproducible in other setup for this kinetic assay. The increase of iNKT cells around day 28, the expression of *il10* and *tnfa* appeared to be similarly up-regulated at the timing. Moreover the expressions of *ccl2* and *cxcl16* appeared to be enhanced in earlier phase (days 14 and 21, respectively), which might be related with the cellular dynamics demonstrated above (Figure 4B).

Administration of α-GC at the immunization ameliorated the cardiac inflammation and fibrosis.

We assumed from above experiments that an administration of α-GC was able to induce cellular responses in the heart presumably via activation of iNKT cells and the involvement of iNKT cells during induction and development of EAMC even in the absence of administration of α-GC. Thus, we attempted to administer α-GC to modulate immune responses against MyHC-α that induce EAMC at the time of immunization according to our previous experiments with EAU.[19] To examine effects of the administration, the acute inflammation induced by immunization with MyHC-α peptide was evaluated on day 21. Control mice showed significant infiltration of inflammatory cells in H&E staining and fibrosis detected as blue-green area in Masson's trichrome staining (Figure 5A. upper panels). On the other hand, α-GC administered mice exhibited the lesser infiltrated cells and smaller areas of fibrosis (Figure 5A. lower panels). The fibrotic area was smaller in α-GC administered mice compared with that of control Figure 5B). When the gene expression was analyzed with the heart at day 21, pro-inflammatory cytokines, *tnfa* and *il6* appeared down-regulated whereas *il10* was in increasing trend (Figure 5C).

To examine the immune responses of T cells obtained from the dLN cells, proliferative response estimated by ³H-TdR incorporation and cytokine production in the culture supernatant with flow cytometer were compared at d 21 after immunization between control and α-GC-treated groups of mice as shown in Figure 5D,E. There was no difference in proliferative responses between two groups (Figure 5D). Although there were differences in the expression of several cytokines in the heart at day 21,
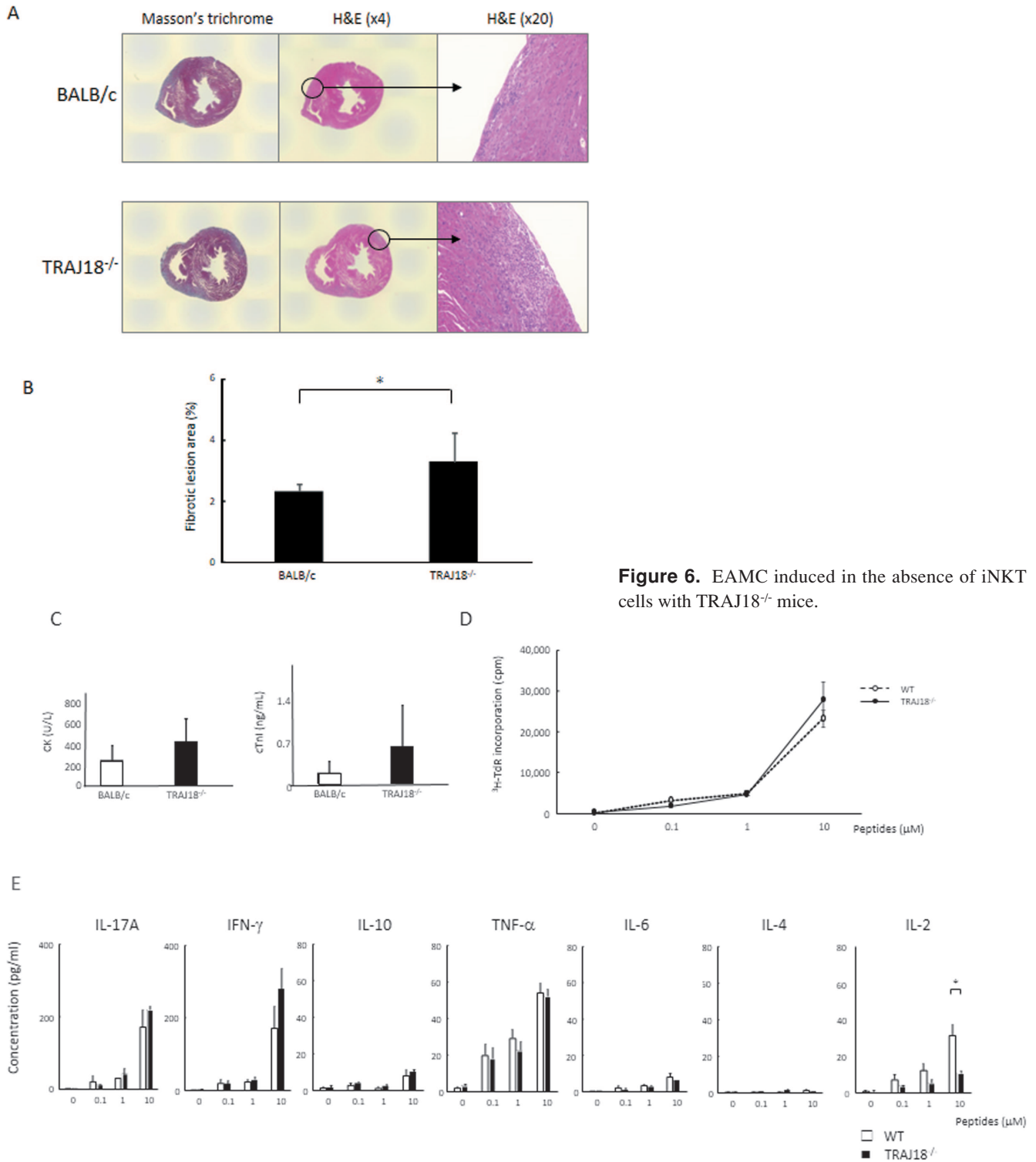
Figure 6. EAMC induced in the absence of iNKT cells with TRAJ18^{-/-} mice.

A. Histopathology of the heart obtained from EAMC-induced WT (BALB/c) and TRAJ18^{-/-} (BALB/c background) mice and stained with Masson's trichrome and H&E solution. Magnification ×4; ×20. In H&E stain, circled area was set to see infiltration of inflammatory cells in the heart tissue. **B**. Histograms of the fibrotic lesion areas. **C**. Quantification of myocardial enzyme and molecules released by inflammatory response. Creatine kinase and cTnI levels were quantified as described in the **Materials and Methods**. **D**. Proliferative responses after 10 days of the primary immunization in WT or TRAJ18^{-/-} mice. The incorporation of ^{3}H-TdR was quantified by scintillation counter. T-enriched cells from dLN of EAMC mice (n = 3 each group) cultured were at each concentration of MyH5 peptide in the presence of APCs as described in Materials and Methods. Prior to the pulse labeling with 3H-TdR, supernatant of each well was collected for quantification of cytokines as shown in **E**. **E**. Cytokine concentration in culture supernatant (pg/ml) was quantified with CBA (cytometric bead array) as described in Materials and Methods. The concentration of indicated cytokines was quantitated in triplicate culture. Representative of two independent experiments with similar results are shown. Graph data are shown as mean ± SD. *P < 0.05

there were no differences in the production of IL-17, TNF-α and IFN-γ at this time point presumably because the main site of T cell activation was in the cardiac tissue (Figure 5E).

Acute inflammatory responses appeared aggravated in TRAJ18^{-/-} mice where iNKT cells were deficient.
If iNKT cells played the beneficial role in mitigating cardiac inflammation, EAMC induction in iNKT-deficient mice may cause deteriorating effect for the cardiac inflammation. Indeed, EAMC induced in TRAJ18^{-/-} exhibited enhanced infiltration of inflammatory cells and aggravated fibrosis compared to those of WT BALB/c mice (Figure 6A). The fibrotic lesion areas were significantly larger than those of WT mice (Figure 6B). Serum level of creatine kinase and troponin I that indicate the tissue damages of the heart appeared higher in TRAJ18^{-/-} mice than those of BALB/c mice (Figure 6C). Meanwhile, when the antigen-specific T cell response was analyzed at day 10 after the primary immunization however, there was no difference in ^{3}H-TdR incorporation between WT and TRAJ18^{-/-} mice at day 10 after immunization (Figure 6D). The cytokine production in the supernatant by the T cells obtained from dLN cells of EAMC-induced WT or TRAJ18^{-/-} cultured in the presence of MyHC-α peptide with APC was examined, the reduced production of IL-2, whereas slightly enhanced production of IFN-γ but not that of TNF-α were noted in TRAJ18^{-/-} mice (Figure 6E).

Discussion

In the present study, the early activation of NKT cells ameliorated EAMC in BALB/c mice when the mice were administered the α-GC with the immunization inoculum. The amelioration appeared to be related the up-regulation of IL-10 and the down-regulation of the expression of pro-inflammatory cytokines, *tnfa* and *il6*. The fibrotic lesion area was reduced in the group that received administration of α-GC at the time of immunization. The finding that iNKT cell may have beneficial effect was reinforced by the finding that EAMC induced in iNKT-cell deficient strain TRAJ18^{-/-} mice in the BALB/c background was aggravated with larger fibrotic lesion areas than those of WT mice.

The administration of α-GC in aqueous solution induced rapid activation of iNKT cells in the heart at day1 that led to the expressions of *Il4*, *Ifng*, and *Ccl2* (Figure 3). The complex formed with the administered α-GC and CD1d was detected on Mϕ but not on Mo with L363 mAb[23] after day 1 of the injection (data not shown), suggesting that the complex on Mϕ stimulated iNKT cells to express *Il4* and *Ifng*, and *Ccl2* to recruit Mo (Figure 3). The response was transient because the NKT cell ligand might have been washed away and disappeared by day 7. When EAMC was induced in the BLAB/c mice without α-GC administration, iNKT cells appeared around days 21－28 along with the development of an inflammatory disease (Figure 4). Because we did not examine CD1d molecules with L363 mAb on Mϕ population, it is not known whether or not there were some endogenous ligands prior to or in concert with activation/proliferation prior to the emergence of iNKT cells, which warrant further investigations. Again the timing of up-regulation of several genes suggests that *Cxcl16* expression on days 14－21 might recruit iNKT cells around day 28 in the usual induction of EAMC; and, therefore, the inflammation was self-limiting in WT mice presumably due to the high expression of IL-10 on day 28 in comparison with other cytokines.

This hypothesis was tested with the use of TRAJ18^{-/-} mice in which iNKT cells were deficient.[16] In those mice with a deficiency of iNKT cells, the beneficial effects represented by the cells accordingly were lost; and, therefore, the development of EAMC could be aggravated. Indeed, the fibrotic lesion areas were enhanced in TRAJ18^{-/-} mice, and myocardial injuries assumed by released creatine kinase and troponin I were higher in TRAJ18^{-/-} mice (Figure 6). Therefore, the hypothesis that iNKT cells may have beneficial effects on the development of EAMC was also confirmed.

Liu et al.[14] demonstrated that α-GC administration ameliorated the EAMC in their previous report. EAMC was induced in BALB/c mice by immunizing with whole protein of porcine cardiac myosin. The mice were administered α-GC intraperitoneally at the time of immunization and injected on alternate days for 6 weeks. The myocardial inflammation improved in the α-GC treated group compared to the control group. They assumed that the NK1.1^{+} iNKT cells and Treg cells were involved with the amelioration with the up-regulation with MMP2 and MMP9 in the heart presumably for the clearance/repair of the inflammatory lesion. Because NK1.1 is not expressed in BALB/c strains of mice, the study remained to be pursued. The present study has clearly demonstrated the involvement of iNKT cells through detection them by not only using real time PCR and flow cytometric analyses but also by using iNKT-deficient mice as a model. Liu et al.'s report implied that Treg cells were involved in the amelioration of EAMC. We have not examined that involvement and will, therefore, pursue that in further investigations. In

TRAJ18^{-/-} mice, the low induction of IL-2 by Ag-specific T-cell response may be related to a dysfunction of Treg cells leading to the enhanced pathology, a topic which also warrants further examination.

In previous studies of AMI and I/R model in mice, α-GC administration also exhibited beneficial effect on cardiac remodeling and function following induction of the diseases with elevated expression of IL-10, an anti-inflammatory cytokine.[12,13] Anti-IL-10 antibody administration abolished the effect of α-GC administration, suggesting that the effect was mediated through production of IL-10 by iNKT cells through the suppression of inflammatory responses. In AMI model, the improvement of cardiac remodeling by IL-10 is mediated by the Mϕ polarization towards M2 and the activation of fibroblast.[24] Besides IL-10, IL-4 has been reported as an amelioration-inducing cytokines in AMI model,[25,26] which seems also reasonable because IL-4 could function as an inducer of type 2 immunity that allows M2-Mϕ accumulation. However, The reports that IL-10 from Mϕ may promote diastolic dysfunction[27] or that IL-4 of eosinophil origin may progress dilated cardiomyopathy[28] also tell us that the specific functions of cytokine does not always bring beneficial outcomes.

Meanwhile, LPCs in the heart are not fully understood that present α-GC to iNKT cells for the induction of IL-10 in models in which beneficial effect has been obtained to date.[13,14] In the present study, we attempted to search candidate for LPCs in the heart by digesting a part of the hearts and found that cardiac Mϕ expressed the highest level of CD1d among CMNC and could serve as LPCs in the heart and were actually shown by L363 mAb that detects α-GC/CD1d complex when mice were exogenously administered the ligand.[23,29] We assumed the possibility from our results that Mϕ is the major and CD1d^{hi} population among cardiac mononuclear cells. However, to test whether the Mϕ is a critical LPC on α-GC administration that exhibits beneficial effects, conditional knockout mice should be employed that carried disrupted alleles of *cd1d1* gene specifically in Mϕ[30,31] in mice of BALB/c background, which remains to be performed.

At least a part of Mϕ obtained from digested cardiac tissue appeared to retain characteristics of primitive Mϕ expressing MHC II[lo] and CX$_3$CR1. Cardiac Mϕ seeded during embryogenesis by yolk sac progenitors and fetal liver seems to have resident-type characteristics but not as fixed as microglia and slowly replaced by blood monocytes,[32-34] and continue to play anti-inflammatory role following pathological state such as ischemic injuries and infections in cardiac micro-environment by bias towards M2-Mϕ or M2-Mϕ-like, reparative Mϕ.[35] Notably, when M1- vs. M2-bias was examined in α-GC-treated vs. vehicle control and in wild type BALB/c mice vs. TRAJ18^{-/-} mice, apparent bias towards M2-Mϕ or reduced M1 proportion were not always observed or did not appear as anticipated manner, although in a steady state, cardiac tissue seems to be protected by a cardiac M2-Mϕ environment.

In summary, iNKT cells exhibit ameliorating function when activated at the time of immunization and the presence of iNKT cell in WT mice appears beneficial in comparison with mice of NKT-deficient strain. The latter finding that TRAJ18^{-/-} mice had aggravated inflammation in the heart implicates that an endogenous ligand in the context of CD1d on Mϕ as LPC stimulate iNKT cells to induce favorable response to reduce inflammatory destruction of myocardium. The cardiac Mϕ appeared CD206^{+} population in steady state and are able to support anti-inflammatory environment as M2-Mϕ. In the present study, α-GC was administered at the immunization period as preventive regimen. Administration of α-GC after immunization preferably after the onset may open further application for treatment of EAMC as a model of human diseases. Employment of specified iNKT cell ligands such as Th1- or Th2-based activity may also be explored for better induction of ameliorating effects via iNKT cells. Therefore, further investigation is warranted because iNKT cell-cardiac Mϕ interaction appears to be a promising target to help prevent or treat myocarditis, and because we have not, so far, been able to trace the long-term outcome more than 60 days after an administration of α-GC on cardiac remodeling.

Acknowledgements

Conflicts of Interest: None

References

1. Aretz HT. Myocarditis: the Dallas criteria. *Hum Pathol* 1987;18: 619-24.

2. Razzano D, Fallon JT. Myocarditis: somethings old and something new. *Cardiovasc Pathol* 2020; 44: 107155.

3. Global Burden of Disease Study 2013 Collaborators. Global, regional, and national incidence, prevalence, and years lived with disability for 301 acute and chronic diseases and injuries in 188 countries, 1990-2013: a systematic analysis for the Global Burden of Disease Study 2013. *Lancet* 2015; 386: 743-800.

4. Levine MC, Klugman D, Teach SJ. Update on myocarditis in children. *Curr Opin Pediatr* 2010; 22: 278-83.

5. Fung G, Lou H, Qiu Y, et al. Myocarditis. *Cir Res* 2016; 118: 496-514.

6. Caforio AL, Pankuweit S, Arbustini E, et al. Current state of knowledge on aetiology, diagnosis, management, and therapy of myocarditis: a position statement of the European Society of Cardiology Working Group on Myocardial and Pericardial Diseases. *Eur Heart J* 2013; 34: 2636-48.

7. Pfeffer MA, Braunwald E. Ventricular remodeling after myocardial infarction. Experimental observations and clinical implications. *Circulation* 1990; 81: 1161-72.

8. Cohn JN. Structural basis for heart failure. Ventricular remodeling and its pharmacological inhibition. *Circulation* 1995; 91: 2504-7.

9. Bendelac A, Savage PB, Teyton L. The biology of the NKT cells. *Annu Rev Immunol* 2007; 25: 297-336.

10. Matsuda JL, Mallevaey T, Scott-Browne J, et al. CD1d-restricted iNKT cells, the 'Swiss-Army knife' of the immune system. *Curr Opin Immunol* 2008; 20, 358-68.

11. Yu KO, Porcelli SA. The diverse functions of CD1d-restricted NKT cells and their potential for immunotherapy. *Immunol Lett* 2005; 100: 42-55.

12. Wu L, Van Kaer L. Natural killer T cells in health and disease. *Front Biosci (Schol Ed)* 2011; 3: 236-51.

13. Sobirin MA, Kinugawa S, Takahashi M, et al. Activation of natural killer T cells ameliorates postinfarct cardiac remodeling and failure in mice. *Circ Res* 2012, 111: 1037-47.

14. Homma T, Kinugawa S, Takahashi M, et al. Activation of invariant natural killer T cells by α-galactosylceramide ameliorates myocardial ischemia/reperfusion injury in mice. *J Mol Cell Cardiol* 2013: 62: 179-88.

15. Liu W, Li S, Tian W, et al. Immunoregulatory effects of α-GalCer in a murine model of autoimmune myocarditis. *Exp Mol Pathol* 2011; 91: 636-42.

16. Ren Y, Sekine-Kondo E, Shibata R, et al. A novel mouse model of iNKT cell-deficiency generated by CRISPR/Cas9 reveals a pathogenic role of iNKT cells in metabolic disease. *Sci Rep* 2017; 7: 12765. doi: 10.1038/s41598-017-12475-4.

17. Eriksson U, Kurrer MO, Schmitz N, et al. Interleukin-6-deficient mice resist development of autoimmune myocarditis associated with impaired upregulation of complement C3. *Circulation* 2003; 107: 320-5.

18. Anzai A, Mindur JE, Halle L, et al. Self-reactive CD4$^+$ IL-3$^+$ T cells amplify autoimmune inflammation in myocarditis by inciting monocyte chemotaxis. *J Exp Med* 2019; 216: 369-83.

19. Satoh M, Namba KI, Kitaichi N, et al. Invariant natural killer T cells play dual roles in the development of experimental autoimmune uveoretinitis. *Exp Eye Res* 2016; 153: 79-89.

20. Epelman S, Lavine KJ, Beaudin AE, et al. Embryonic and adult-derived resident cardiac macrophages are maintained through distinct mechanisms at steady state and during inflammation. *Immunity* 2014; 40: 91-104.

21. Satoh M, Hoshino M, Fujita K, et al. Adipocyte-specific CD1d-deficiency mitigates diet-induced obesity and insulin resistance in mice. *Sci Rep* 2016; 6: 28473. doi: 10.1038/srep28473.

22. Hamad M, Klein JR. Phenotypic and functional heterogeneity of murine intestinal intraepithelial lymphocytes defined by cell density: implications for route of differentiation and responsiveness to proliferation induction. *Immunology* 1994; 82: 611-6.

23. Yu ED, Giradi E, Wang J, et al. Structural basis for the recognition of C20:2-αGalCer by the invariant natural killer T cell receptor-like antibody L363. *J Biol Chem* 2012; 287: 1269-78.

24. Jung M, Ma Y, Iyer RP, et al. IL-10 improves cardiac remodeling after myocardial infarction by stimulating M2 macrophage polarization and fibroblast activation. *Basic Res Cardiol* 2017; 112: 33. doi: 10.1007/s00395-017-0622-5.

25. Shiraishi M, Shintani Y, Shintani Y, et al. Alternatively activated macrophages determine repair of the infarcted adult murine heart. *J Clin Invest* 2016; 126: 2151-66.

26. Shintani Y, Ito T, Fields L, et al. IL-4 as a repurposed biological drug for myocardial infarction through augmentation of reparative cardiac macrophages: Proof-of-concept data in mice. *Sci Rep* 2017; 7: 6877. doi: 10.1038/s41598-017-07328-z.

27. Hulsmans M, Sager HB, Roh JD, et al. Cardiac macrophages promote diastolic dysfunction. *J Exp Med* 2018; 215: 423-40.

28. Diny NL, Baldeviano GC, Talor MV, et al. Eosinophil-derived IL-4 drives progression of myocarditis to inflammatory dilated cardiomyopathy. *J Exp Med* 2017; 214: 943-57.

29. Wei Y, Zeng B, Chen J, et al. Exogenous bacterial glycolipids are required for the generation of natural killer T cells mediated liver injury. *Sci Rep* 2016; 6: 36365. doi: 10:1038./srep36365.

30. Bai L, Constantinides MG, Thomas SY, et al. Distinct APCs explain the cytokine bias of α-galactosylceramide variants *in vivo*. *J Immunol* 2012; 188: 3053-61.

31. Clausen BE, Burkhardt C, Reith W, et al. Conditional gene targeting in macrophages and granulocytes using LysMcre mice. *Transgenic Res* 1999; 8: 265-77.

32. Pinto AR, Ilinykh A, Ivey MJ, et al. Revisiting cardiac cellular composition. *Circ Res* 2016; 118: 400-9.

33. Swirski FK, Robbins CS, Nahrendorf M. Development and function of arterial and cardiac macrophages. *Trends Immunol* 2016; 37: 32-40.

34. Ginhoux F, Guilliams M. Tissue-resident macrophage ontogeny and homeostasis. *Immunity* 2016; 44: 439-49.

35. Epelman S, Lavine KJ, Beaudin AE, et al. Embryonic and adult-derived resident cardiac macrophages are maintained through distinct mechanisms at steady state and during inflammation. *Immunity* 2014; 40: 91-104.